

NASA Contractor Report 3484

# Critical Requirements for the Design of Large Space Structures

John M. Hedgepeth

CONTRACT NAS1-15347  
NOVEMBER 1981

**NASA**

NASA Contractor Report 3484

# Critical Requirements for the Design of Large Space Structures

John M. Hedgepeth  
*Astro Research Corporation*  
*Carpinteria, California*

Prepared for  
Langley Research Center  
under Contract NAS1-15347



National Aeronautics  
and Space Administration

**Scientific and Technical  
Information Branch**

1981

## TABLE OF CONTENTS

SUMMARY . . . . .	1
INTRODUCTION . . . . .	1
OVERVIEW . . . . .	2
OPERATIONAL LOADS . . . . .	4
STIFFNESS REQUIREMENTS . . . . .	8
Structure-Control Interaction . . . . .	9
Deformations . . . . .	12
Remarks . . . . .	15
PRECISION REQUIREMENTS . . . . .	16
MEMBER SLENDERNESS . . . . .	18
DESIGN EXAMPLES . . . . .	21
Truss Antenna Reflector . . . . .	21
Interorbit Propulsion Loads . . . . .	22
Free-Flying Solar Reflectors . . . . .	23
CONCLUDING REMARKS . . . . .	23
REFERENCES . . . . .	24
APPENDIX: FLEXIBLE-STRUCTURE ANALYSES . . . . .	37

## LIST OF ILLUSTRATIONS

Figure 1.-	Equivalent loading pressure versus orbital altitude . . . . .	25
Figure 2.-	Equivalent angular acceleration versus orbital altitude . . . . .	26
Figure 3.-	Required frequency ratio for stability for a center-body controlled spacecraft with flexible appendages . . . . .	27
Figure 4.-	Deformations due to attitude control . . . . .	28
Figure 5.-	Deformations due to lateral acceleration . . . . .	29
Figure 6.-	Potential antenna sizes for $w_{rms} = \lambda/100$ as limited by fabrication imperfections . . . . .	30
Figure 7.-	Potential tetrahedral truss antenna size for $w_{rms} = \lambda/100$ as limited by thermal strains . . . . .	31
Figure 8.-	Tetrahedral truss configuration . . . . .	32
Figure 9.-	Effect of out-of-straightness on axial stiffness . . . . .	33
Figure 10.-	Allowable member slenderness . . . . .	33
Figure 11.-	200-m-diameter deployable antenna . . . . .	34
Figure 12.-	Mass and stowage ratio for tetrahedral truss. . . . .	35
Figure 13.-	Baseline configuration of a solar- reflector spacecraft . . . . .	36

## SUMMARY

The future promises large structures which must be deployed, erected, assembled, or fabricated in space. Such structures will be designed to deal with phenomena as primary criteria which have been considered as only secondary in the past. The purpose of this paper is to discuss these spaceflight design requirements. The conclusion is reached that for most situations, the primary requirements will arise from the demands for high dimensional accuracy of the structure throughout its long useful life.

## INTRODUCTION

The successful performance of any structure depends largely on the identification of the critical or primary loads and design criteria on which the design is based. Until now, most structures used in spaceflight have been designed primarily to withstand launch loads. A great deal of effort was exerted in the 1960's to understand these loads and to develop criteria for design that would yield structures that could withstand the loads without being excessively heavy. The design process for launch structures has therefore matured on this solid foundation of recognized design criteria.

Most "space" structures have, in fact, been "launch" structures, inasmuch as their primary design requirements have stemmed from the launch environment. The future, however, promises large structures which must be deployed, erected, assembled, or fabricated in space. Indeed, their primary design requirements will be derived from the spaceflight environment and will deal with phenomena as primary criteria which have been considered as only secondary in the past. The design of such genuine "space" structures will require a similarly solid foundation of critical criteria as has been created for the launch environment.

The proper selection of critical design requirements is not only necessary for the actual design of structures, it is also necessary for the preliminary study of missions and concepts so that realistic structural data can be generated for cost and feasibility analyses and for the determination of technology readiness. Indeed, the validity of future mission planning and the adequacy of technology-development programs depend heavily on the correctness of the design criteria. This is particularly true of many of the envisioned missions in which the large structure dominates the spacecraft design.

The present study was undertaken to examine critical design criteria for large space structures. The objective was to identify and establish critical baseline design requirements for general types of structures by a series of rational parametric analyses. The results should improve the basis for future space structures system and technology efforts. They will also add to the needed solid foundation of design criteria.

Much of the results of the investigation has been reported in references 1 through 6. The present report constitutes a summing up of the investigation and an exposition of its major conclusions.

## OVERVIEW

The rational design of all structures must start with a definition of the task or function of the structure. The task of a flight structure is generally to enclose, protect, support, and/or otherwise provide the desired environment for a payload. For each application, a large number of detailed requirements exists, which, if taken collectively, expresses the means by which the proper performance of the structure's task can be met. Usually a small subset of these requirements dominates the design and is hence termed "primary." The other "secondary" requirements are checked a posteriori and changes (usually slight) are made to accommodate them.

If the structure is a launch structure that is subsequently also used in space, then strength often dominates, and primary design requirements are similar to launch-based experience. For true space structures erected/fabricated/deployed in orbit, the environment in space is quite benign, the applied loads are apt to be small, and the strength of the structure is not a pacing factor. On the other hand, the demands of antennas and solar reflectors for accurate positioning and the requirements of adequate stiffness to avoid undesirable structural distortions are often serious and thereby dictate the design.

For deployed and assembled space structures, another primary requirement is that the structure must be packaged in the available volume for transport to space. In the past, the need for compact packaging has usually been more difficult to satisfy than the need for low weight. The Shuttle offers a great deal more space, but constraints will always be present.

Those who utilize deployable structures on their spacecraft have universally insisted that the structures be tested before flight by deploying them on the ground. Various means have been devised to counteract the forces of gravity and to provide sufficient area to allow deployment. This ground testing is likely to remain a primary requirement until Shuttle-based testing techniques can be devised. Even then, ground testing will be required to the extent practicable and will usually constitute the highest loading environment.

Reliability and cost are important factors in a design. Experience has shown that both factors are closely related to the ground testing. Thus, the reliability is demonstrated primarily through ground testing and most of the recurring and nonrecurring costs are associated with ground testing. This situation is not expected to change until a great amount of experience with space operations allows a change in basic program philosophy.

Damage tolerance is clearly a requirement. Large expanses of statically determinate structure with thin members may have an unacceptably high probability of failure due to meteoroid damage. Even if the structure were redundant, the degradation in precision caused by local damage must be considered. Structures involved in manned operations or with docking, assembly, and refurbishment phases must be designed so that malfunction of other subsystems is unlikely to cause loss of structural integrity.

Identification of critical design requirements requires consideration of the five phases in the life of a space structure:

- Prelaunch
- Launch
- Interorbit boost
- Erection in space
- Space operation

The prelaunch phase influences the design primarily through the requirements on fabrication accuracy and ground test. The launch phase influences the packaged configuration. Interorbit boost can cause major design loads if the structure is previously erected. The integrity of the partially erected structure (whether deployed, assembled, or fabricated) must be assured.

Finally, the structure must furnish secure and precise support to the payloads during the long operational phase. Indeed, the most basic requirement is that the structure must interface "happily" with its payload and the other parts of the system. The requirements of dimensional precision and high stiffness (which go hand in hand) are very important.

#### OPERATIONAL LOADS

Attention should be paid first to the requirements which arise during the operational phase of the mission. In fact, the

most desirable situation would be one in which the primary design criteria are derived from the operational requirements. Certainly the operational requirements are necessary if not sufficient.

Common to all spacecraft are the loads encountered in operation. A conservative quantitative estimation of some of these loads in Earth orbit was presented in reference 7. Those results are repeated in Figure 1 with some additions. They include the most severe loads that can be expected from normal, unmanned operation. They do not include loads due to special rapid-slewing maneuvers, overly robust control torquers and thrusters, and internally generated loads arising from on-board activities.

In Figure 1, the loads are shown in the form of effective pressure as a function of orbital altitude. The two basic environmental loads are air drag, which is dominant at the lower altitudes, and solar pressure, which is constant at its 1-AU value for specular reflection of  $0.9 \times 10^{-5} \text{ N/m}^2$ . Other environmental forces have been considered and shown to be many orders of magnitude less severe. They are

- Solar wind
- Electrostatic and electromagnetic forces due to spacecraft charging
- Average micrometeoroid flux

For a recent detailed treatment of many of these effects, see Chapter V of reference 8.

The other loads shown in Figure 1 are inertia-type loads which are dependent on the areal mass density of the spacecraft. The effective pressure due to station-keeping adjustment is also dependent on the ratio of the needed plane-change angle to the allowed angular duration of thrusting. The curve shown is for  $m_a \alpha/\theta = 10^{-4} \text{ kg/m}^2$  which applies, for example, to a plane change  $\alpha = 1 \text{ mrad}$ , a thrusting duration of  $\theta = 1 \text{ rad}$ , and a mass per unit area  $m_a = 0.1 \text{ kg/m}^2$ .

Gravity gradients and angular accelerations produce effective pressures which are proportional to the areal mass density and the distance  $r$  from the center of gravity of the spacecraft. The relative contribution of various effects are seen most clearly by examining their equivalent angular accelerations given in Figure 2. The curve for gravity gradient, for example, is obtained from any of the gravity-gradient curves in Figure 1 by dividing by its  $m_a r$ .

The results for fixed-site tracking give the maximum angular acceleration experienced by a satellite controlled to point at a ground target as it passes overhead. The analysis is similar to that given in reference 7 for the angular acceleration of a solar-reflecting satellite controlled to keep the reflected rays aimed at a ground site. The fixed-site-pointing accelerations turn out to be exactly twice as much as the planar solar-reflecting ones.

In the case of the solar-reflecting satellite, the value of the maximum attitude acceleration can be higher than those for the planar case when the more intricate three-dimensional mission is analyzed. Actually, the motions can become very large as the spacecraft endeavors to keep the reflected Sun's rays directed at the ground site. As is pointed out in reference 7, however, most cases are covered if the acceleration is limited to ten times the value obtained by the planar analysis. The order-of-magnitude spread is indicated by the bar at an orbital altitude of 4000 km.

The Solar Maximum Mission spacecraft is the first of many low-orbit satellites which are expected to make use of the TDRSS satellites in geosynchronous orbit to maintain a continuous high-data-rate link to ground. The maximum angular acceleration of the high-gain antenna on that spacecraft is indicated in Figure 2.

If a satellite in noncircular orbit is required to remain pointed at the Earth's center, then angular accelerations will occur. The values of these accelerations are seen to be lower

than the others even for the highly eccentric 12-hour orbit, often termed "Molniya" after the Soviet spacecraft which made early use of this orbit.

The effective pressure loadings shown on Figure 1 are therefore the highest loads that can be expected in normal unmanned operation. They are small when compared to terrestrial loadings. For example, a dynamic pressure of  $0.01 \text{ N/m}^2$  is produced by a speed of only 12.5 cm/s at sea level. This same value of load/area (which is the upper limit of the graph in Figure 1) is less than one hundredth of the weight of an ordinary sheet of paper 0.1-mm thick. For many space structures, the loads are so small that they do not form primary criteria.

For some situations, the operational loads do supply the basis of primary criteria. The structure of the solar-reflecting spacecraft (ref. 7 and, more recently, ref. 9) is designed to supply sufficient tension to the circular reflector membrane to keep the slope at the boundary due to a pressure of  $10^{-5} \text{ N/m}^2$  to 1 mrad. The resulting internal structural loads are not inconsiderable, having values of hundreds of Newtons in the rim, for example.

Similarly, for low orbits and large structures, the air drag and gravity-gradient loads may pose primary design constraints. In reference 10, for example, the column loads in members of a tetrahedral truss are calculated for a worst-case gravity-gradient loading. Values of thousands of Newtons were obtained for kilometer-sized structures.

Finally, the loads due to operating installed equipment may cause severe design problems. The following table, taken from Page 620 of reference 8, contains some examples:

SOURCE OF DISTURBANCE	AMPLITUDE RANGE	FREQUENCY RANGE (Hz)
CMC imbalance	0.01 to 10 N	10 to 50
Reaction wheel imbalance	0.001 to 1 N	1 to 50
Reaction wheel bearing noise	0.0001 to 0.01 N	1 to 500
Solar-array drive torque	0.001 to 0.01 N-m	0.001 to 0.1

To these must be added transient loads due to manned activities, docking maneuvers, and control jets. Some of the tabulated loads are of particular concern, not because of their amplitude, but because of their high frequency. Avoiding resonance with natural structural vibrations could be very difficult. The treatment of the loads for a specific mission is given in Chapter 1 of reference 11.

#### STIFFNESS REQUIREMENTS

The stiffness requirements for space structures arise from two basic causes:

- The structure must be stiff enough to avoid undesirable interaction with closed-loop control systems.
- The structure must be stiff enough to withstand the various disturbing forces without suffering unacceptable distortions.

Ordinarily, the stiffness of a spacecraft is expressed in terms of its natural frequency. That same approach is adopted in this paper even for situations wherein the external loading can be considered to be applied statically.

Control-system technology has become very sophisticated and can be expected to become much more so in the future. However, assuring satisfactory operation by means of feedback control can be expensive, the cost increasing as the natural frequency decreases. The approach taken herein is to seek criteria which

would avoid unnecessary added complexity of the control system due to the structure flexibility. Thus, the coupling between the structure and the control system is minimized and the interface-management problem is greatly simplified.

### Structure-Control Interaction

Unstable interaction between the structural deformation and a closed-loop control system can be avoided if the effect of the flexibility is low enough to keep the total gain of the feedback loop less than unity. This so-called "gain stabilization" principle is well known. It is conservative because stability is often achieved by proper phasing even if the gain exceeds unity.

The required stiffness for gain stabilization can be expressed in terms of the ratio between the structural natural frequency and the control frequency. This control frequency is defined by noting that the control system acts essentially as a centering spring that overcomes a steady disturbing torque  $Q$  with an allowable angular displacement  $\Delta\theta$ . The effective stiffness of the control system is then

$$K = \frac{Q}{\Delta\theta} \quad (1)$$

and the control frequency is

$$f_c = \frac{1}{2\pi} \sqrt{\frac{K}{I}} \quad (2)$$

where  $I$  is the mass moment of inertia of the spacecraft about the same axis as the torque is applied.

The structural natural frequency depends not only on the stiffness and the mass distribution, but also on the boundary conditions. Since spacecraft are almost always free bodies, one is tempted to use the natural frequency obtained with free-free

boundary conditions. Because most flexible spacecraft structures flown up to the present have been appendages to central spacecraft, the present practice is to work with the cantilever frequency. In this paper, the same practice is employed. In particular, the natural frequency is defined as the fundamental frequency that results from rigidly supporting the center of the spacecraft in displacement and rotation. This definition not only has the advantage of continuity with the past, but also makes the description of the stiffness independent of whether the phenomenon being considered is symmetric or antisymmetric. Note, however, that when the flexible structure becomes the dominant part of the spacecraft, the use of free-free boundary conditions will be more appropriate.

The conditions for gain stabilization are studied in reference 12. The results of that analysis show the influence of the structural damping coefficient  $\zeta$  (equal to the reciprocal of the maximum resonant amplification factor) and control-system rolloff on the required ratio of natural cantilever frequency  $f_n$  to control frequency  $f_c$ . The structural configuration is shown in Figure 3. It consists of a center body with flexible arms supporting a tip mass. The control torque is applied to the center body and the angular error is also sensed there. Example results are given in Figure 3 for an assumed first-order (6 dB/octave) rolloff filter. The plot shows the variation of  $f_n/f_c$  with the ratio of the moment of inertia of the sprung body  $I_2$  to the center-body moment of inertia  $I_1$  for several values of damping  $\zeta$ . A value of  $\zeta = 0.003$  is appropriate to pure materials damping, whereas  $\zeta = 0.1$  applies to a built-up structure with mechanical joints. Note that when the inertia of the sprung body dominates, the cantilever natural frequency can be less than the control frequency. (Note, however, that the free-free frequency is always greater than  $f_c$ .) For intermediate values of inertia ratio, the frequency ratios are modest even for low damping.

The results in Figure 3 are determined with the equation from reference 12 for the required frequency ratio

$$\left(\frac{f_n}{f_c}\right)^{2+r} = \frac{I_2/I_1}{(1+I_2/I_1)^{(3+r)/2}} \frac{1}{\zeta} \quad (3)$$

where  $r$  is the order of the rolloff filter. More recently, the same type of analysis has been applied to the control of a uniform beam (or plate) with control forces applied at the center or at the tips and with the angular error sensed as the slope at the center or the slope of the line between the tips. The results, as derived in the Appendix, are

$$\left(\frac{f_n}{f_c}\right)^{2+r} = \frac{C_1}{(19.2)^{(3+r)/2}} \frac{1}{\zeta} \quad (4)$$

where  $C_1$  is given by the following table

TORQUING		
	CENTER	TIP
SENSING		
Center	9.7	3.6
Tip	3.6	1.333

The important influence of control-component location is clearly seen.

The determination of the required control frequency itself is a separate matter. For large structures in a planetary orbit, the dominant disturbing torque is that arising from gravity gradient. If the worst-case attitude is assumed for the platform configuration, then the control frequency can be estimated from Eqs. (1) and (2) to be

$$f_c = \frac{1}{2\pi} \sqrt{\frac{3k}{2R^3 \Delta\theta}} \quad (5)$$

where R is the orbital radius and

$$k = 3.984 \times 10^{14} \text{ m}^3/\text{s}^2$$

Some example resulting values of control frequency are:

ORBIT	ACCURACY	$f_c$ , Hz
LEO (H = 270 km)	0.1°	0.0053
GEO	0.1°	0.00034
LEO	1 arc s	0.10
GEO	1 arc s	0.0064

As a comparison, the vernier control system of the Space Shuttle, with a long boom attached, was modeled several years ago (see ref. 12). The resulting control frequency was approximately 0.009 Hz, which is reasonable agreement with the LEO, 0.1° value in the table.

#### Deformations

If the disturbing forces were distributed over the spacecraft so that they were proportional to the mass distribution, then the structure would accelerate through space as a rigid body with the resulting d'Alembert inertia forces cancelling the disturbing forces. No distortion would occur. Usually, however, the distributions are different and distortion occurs. This is especially true if the loads are concentrated.

A major source of concentrated disturbance loads is the control system. As an example, consider a large planar platform in circular orbit, controlled by gas jets at the boundary (see

Figure 4). For either the circular or rectangular planform, the control forces will cause an angular acceleration  $\ddot{\theta}$  which, in turn, generates the balancing inertia loads. The distortion can be expressed as the rms deviation from a planar surface  $w_{\text{rms}}$ . Analysis in the Appendix shows that the ratio of the rms distortion to the characteristic dimension can be expressed as

$$\frac{w_{\text{rms}}}{D} = \Gamma_{\theta} \frac{\ddot{\theta}}{f_n^2} \quad (6)$$

where  $f_n$  is the cantilever natural frequency (with the structure assumed clamped at its centerline) and  $\Gamma_{\theta}$  is a constant which depends on the planform.

$$\begin{aligned} \Gamma_{\theta} &= 0.00214 \quad , \text{ circular} \\ &= 0.00095 \quad , \text{ rectangular} \end{aligned}$$

Solving for the required natural frequency in terms of the allowable distortion gives

$$f_n = \sqrt{\Gamma_{\theta} \frac{\ddot{\theta}}{w_{\text{rms}}/D}} \quad (7)$$

The allowable amount of distortion is a function of the mission. For radiofrequency antennas, the allowable distortion can be related to the antenna performance. A simplified investigation is given in Chapter 2 of reference 11.

For gravity-gradient loading at LEO, let  $\ddot{\theta} = 4 \times 10^{-6} \text{ rad/s}^2$  (from Figure 2) and take  $w_{\text{rms}}/D = 10^{-5}$  for a circular narrow-beam antenna. Then, the natural frequency would be required to be

greater than 0.03 Hz. In this example, the requirement for limiting deformation is more stringent than the requirement for avoiding structure-control instability.

The example can be extended. Suppose that the control jets are sized large enough to have only a 10-percent duty factor when resisting the gravity-gradient disturbances. Include a dynamic response factor of 1.5 to account for the transient dynamic overshoot during the jet turn-on. The angular acceleration  $\ddot{\theta}$  is increased by a factor of 15. Then the required natural frequency would be 0.12 Hz.

An even more stringent requirement results if the antenna must be slewed to track a ground target. A value of  $\ddot{\theta} = 10^{-4}$  (see Figure 2) would be necessary at an altitude of 650 km and require a natural frequency of 0.15 Hz.

Note that these requirements are independent of antenna size. Of course, the small desired relative deformation implies a large antenna. In addition, the problem of meeting the requirement becomes more severe with large antennas.

Trajectory-modification thrusting can be analyzed in much the same manner. In this case, the requirement on natural frequency is (see Figure 5) obtained in the Appendix to be

$$f_n = \sqrt{\Gamma_Z \frac{\ddot{z}}{w_{rms}}} \quad (8)$$

where

$$\begin{aligned} \Gamma_Z &= 25.1 \times 10^{-3} && , \text{ circular} \\ &= 12.2 \times 10^{-3} && , \text{ rectangular} \end{aligned}$$

As an example, consider the station-keeping case shown in Figure 1 in which a 1-mrad plane change is accomplished over

1 rad of orbit. The acceleration at LEO and GEO is 0.009 and 0.00023 m/s<sup>2</sup>, respectively. Assume the desired limitation on  $w_{rms}$  is 1 mm. Then for the circular planform, the required natural frequency is 0.47 Hz at LEO and 0.076 Hz at GEO. If a dynamic response factor of 1.5 is included, the required frequencies become 0.58 and 0.093 Hz at LEO and GEO, respectively.

Another phenomenon of concern is the situation in which the flexible structure can tolerate large distortions but it is attached to a center body which must point with high accuracy. The concern is with the effect of the residual oscillations of the flexible appendage on the attitude of the center body. Assume that the oscillations are induced by a transient acceleration of the spacecraft (for example, a slewing maneuver) of  $\ddot{\theta}$ . After the transient acceleration is removed, the residual oscillation of the center body has an amplitude  $\theta_1$  which must be kept small. The required cantilever natural frequency of the appendage can be shown to be

$$f_n^2 = \frac{1}{2\pi^2} \frac{I_2/I_1}{1+I_2/I_1} \frac{\ddot{\theta}}{\theta_1}$$

where  $I_1$  and  $I_2$  are the moments of inertia of the center body and appendage, respectively.

As an example, let  $\theta_1 = 1$  arc s and  $\ddot{\theta} = 10^{-6}$  rad/s<sup>2</sup> (see Figure 2). Then for an inertia ratio  $I_2/I_1$  of 0.1, the required natural frequency is 0.03 Hz. Note that appendages, although they are usually relatively small in mass, have appreciable moments of inertia because of their large radii of gyration.

#### Remarks

The examples given herein are arbitrarily chosen, but are representative of situations which can be expected to occur. It

is evident that the stiffness requirements are most likely to arise from the necessity of small deformations rather than in order to avoid undesirable interaction with the control system.

#### PRECISION REQUIREMENTS

Many of the possible missions involving large space structures will require very high precision in the structural geometry. Not only must the structure be stiff enough to avoid unwanted distortions, but also the structure must be constructed accurately and in such a way as to retain its accuracy during the long exposure to the variable temperature, ionizing radiation, high-vacuum space environment. Of course, careful adjustment in space during erection and meticulous maintenance is one possible strategy to follow. But a great deal of time, money, and complication can be avoided if the precision requirements could be met without adjustment in space and without maintenance.

The feasibility of such an approach has been the subject of a major investigation during the past 3 years. Much attention was devoted to the estimation of the effect of unavoidable tolerance errors in the dimensions of individual structural elements on the accuracy of the overall structure. This investigation was aided by the discovery, reported in reference 2, of a powerful equivalence principle linking the analyses of errors to that of vibration frequencies. The application of this principle to various types of antenna structures is reported in reference 3. The conclusion is summarized in Figure 6 taken from that reference.

In Figure 6, the achievable size  $D$  of an antenna, measured in radiofrequency wavelength  $\lambda$ , is plotted versus the rms value of the unit length error of the structural elements. The rms distortion of the antenna surface is taken to be  $\lambda/100$  and the results apply to a ratio of focal length to structural diameter

of two. The curves show that the truss structure is most attractive and that  $D/\lambda = 10,000$  is possible for a fabrication-error parameter of  $10^{-5}$ , which should be obtainable with careful tooling without inordinate cost.

Not only must the structure be erected accurately, but also it must remain accurate. Therefore, attention was given to the effects of thermal strains which are expected to be the major contributor. The analysis is reported in reference 3 and the results summarized in Figure 7 taken from that reference. Here, the ratio  $D/\lambda$  is plotted against the parameter  $\alpha T_{\max}$ , where  $\alpha$  is the thermal-expansion coefficient and  $T_{\max}$  is the maximum equilibrium temperature. Only the deep-truss type of structure was analyzed. Otherwise, the particulars are the same as those in Figure 6. For a value of  $\alpha T_{\max}$  of  $10^{-4}$ , a  $D/\lambda$  of 4000 is achievable unless the Sun is almost tangent to the surface.

The conclusion is that very precise structures are possible at reasonable cost and constructed of reasonable materials. Such precision is possible because the structures are designed to be deep enough to avoid the magnified surface errors that come from shallow configurations. In addition, the cellular nature of the truss contributes to the precision by allowing the random length errors in the individual members partially to cancel out. Thus, with reference to Figure 8, the reasons for the high accuracy are that  $\ell$  is much smaller than the overall size  $D$  of the structure and that  $H$  is greater than or equal to  $\ell$ . See references 1 and 2 for details.

The projections are based on being able to maintain tolerances in the fabrication of the individual members to one part in 100,000. This means that a 10-m-long member would be made accurately to 0.1 mm, for example. Such precision should be possible with careful joint design and appropriate fabrication tooling and procedures.

Finally, the materials used in the structure must have excellent dimensional stability. The deepness of the structure keeps the demands on material performance to reasonable levels, but the effects of differential thermal strains and long-time changes must be kept to a few parts per million.

#### MEMBER SLENDERNESS

The operational loads in well-designed (deep) space structures are so small that the members sized to carry the resulting internal loads are likely to be very slender. Realistic sizing must therefore come from other considerations discussed in the following.

An important criterion arises from the fact that the axial stiffness of a strut is severely degraded if it is not straight. As seen in Figure 9, the reduction in stiffness is a function of the ratio of the crookedness  $\delta$  to the radius of gyration  $k_c$  of the cross section. The equation shown in the figure applies to a sinusoidal deformation shape. Other shapes such as constant-curvature and gravity-sag shapes yield closely similar results.

In order to maintain the loss in axial stiffness to 5 percent, let the crookedness  $\delta$  be set at less than  $k_c/3$ . For a thin-walled tube, the ratio between  $\delta$  and the diameter  $d$  must be less than about 1/10.

Such straightness demands are easy to meet for ordinary proportions. As the slenderness ratio of strut length  $l$  to  $k_c$  increases, however, practical difficulties arise. The consequences of some of these difficulties are shown in Figure 10.

As previously remarked, ground testing will be required. In order to avoid the complications of supporting each strut at interior points against gravity sag, the gravity deflection

$$\delta = \frac{5}{384} \frac{\rho g l^4}{E k_c^2}$$

must be kept small enough. For material properties appropriate to graphite composites,

$$E = 1.1 \times 10^{11} \text{ N/m}^2$$

$$\rho = 1520 \text{ kg/m}^3$$

the slenderness limitation given on the first line of the figure must be observed.

Measuring the crookedness of slender fabricated members is a well-known problem. While testing in a horizontal position in a water tank is a possible approach, questions always arise about the effects of the supports on the validity of the data. And the process is time-consuming and expensive. A preferable approach would be to suspend the strut vertically for measurement. In order that the data be valid, the ratio of gravity-induced load to Euler load

$$\frac{P}{P_{Eu}} = \frac{\rho g l^3}{\pi^2 E k_c^2}$$

must be small. This results in the criterion on the second line of Figure 10.

The third criterion arises from the difficulty of fabricating the member with enough straightness. Too stringent a requirement could result in a high rejection rate. The rise height of a fabricated member would be

$$\delta = \frac{l^2 \Delta \epsilon}{8k_c}$$

where  $\Delta\varepsilon$  is the differential strain error arising, for example, from nonuniformities of material properties or curing temperatures in a distance  $k_c$  across the cross section.

When the struts are assembled into a redundant structure, the length imperfections will induce residual loads in the struts. This phenomena is treated in reference 1. The conclusion is that the rms residual load strain is equal to the rms unit member length imperfection  $\sigma_\varepsilon$  divided by  $\sqrt{3}$ . The ratio of the rms member load to its Euler load is

$$\frac{P_{\text{rms}}}{P_{\text{Eu}}} = \frac{\sigma_\varepsilon}{\sqrt{3} \pi^2} \left( \frac{\ell}{k_c} \right)^2$$

The resulting limitation is given in the fourth line of Figure 10. As a final example of slenderness limitation, the natural vibration frequency of the member should be higher than that of the structure as a whole. For a pin-ended member and a free-free truss with square planform (see ref. 10), the ratio of the strut and truss natural frequencies is

$$\frac{f_{\text{strut}}}{f_{\text{truss}}} = 3.43 \sqrt{\left( 1 + \frac{m_p}{m_s} \right)} k \frac{L^2 k_c}{H \ell^2}$$

where  $m_p/m_s$  is the ratio of the payload mass to the structural mass and  $k$  is the joint-mass factor. The resulting slenderness criterion is shown on the last line of Figure 10.

Comparison of these limitations shows that ground testing requirements could predominate. If these are accounted for in some other fashion, then the residual-load criterion would be the most severe.

## DESIGN EXAMPLES

The application of the foregoing loads and criteria to the design of the spacecraft structure depends strongly on the mission. Some examples are given in references 3, 4, 5, and 9. The salient features of these studies are discussed herein. See the references for a more detailed description.

### Truss Antenna Reflector

Knitted metallic mesh as a reflector surface has the advantage that it is lightweight ( $\sim 60 \text{ g/m}^2$ ) and stows compactly. It has the disadvantage that it is structurally a membrane, and therefore cannot be shaped locally into a paraboloidal surface. Therefore, the antenna surface must consist of a large number of facets that are small enough that the departure of the membrane surface from the desired paraboloid is acceptably small. This requirement is found in reference 3 to dictate the texture of the structural design if tedious adjustment on assembly is to be avoided.

The depth of the truss  $H$  is selected in reference 4 to be equal to the facet size  $\ell$  (see Figure 8) in order to achieve good precision without making the intersurface (core) members overly long.

The cross section of the members is sized so that the membrane tensions in the reflector mesh are handled without excessive local deflection of the struts as discussed in reference 4. Incidentally, the required value of mesh tension is established in order to assure good filament-to-filament conductivity in the mesh. If the reflector surface were a foil, the minimum tension would be established by the need for smoothing the folds in the stowed film. An initial study of this problem is reported in Chapter 3 of reference 11.

The foregoing process allows the determination of designs for various sizes and focal lengths. A particular design for a 200-m-diameter reflector with a focal length of 400 m is shown in Figure 11.

The following points are noted:

- The local design loads due to mesh accuracy requirements are much higher than any of the operational loads.
- The natural frequency is amply high to furnish the required stiffness.
- The member slenderness ratio is  $\ell/k_c = 490$ . This value is not too far from the limitations<sup>c</sup> of Figure 10.
- The structure is highly redundant so that meteoroid damage should not endanger structural integrity. Such damage could deteriorate the accuracy. An initial analysis of meteoroid damage is given in Chapter 4 of reference 11.

Clearly, refinement of the design will yield changes. But they can be expected to be of secondary nature. Therefore, the requirements of adequate reflector surface precision are the primary design requirements.

#### Interorbit Propulsion Loads

If the erected truss structure described in Figure 11 is moved from one orbit to another, the loads caused by the acceleration will require greater local member strength. The effect of interorbit propulsion loads on the design of truss antenna structures is investigated in reference 4. Figure 12 shows some of the results of that study. Clearly, if accelerations of  $1 \text{ m/s}^2$  are desired, the effect on the design is profound. The interorbit propulsion requirement should then be treated as the primary requirement. The entire design configuration should then be reexamined in light of the added requirement. For example, external bracing could lower the influence drastically. The large mass and package-volume increases could therefore be avoided.

## Free-Flying Solar Reflectors

The design of large reflecting satellites, which are essentially flat membrane mirrors, requires a structure which can hold the boundary of the membrane in a plane. The structure must also supply enough tension to the membrane to prevent excessive slopes in the membrane due to the predominant force of solar pressure. The structure designed to do those tasks is shown in Figure 13.

Salient points are:

- The design furnishes adequate strength resistance to environmental forces.
- The natural frequency of the membrane (which is a dominant mass element) is 0.03 Hz. For a design altitude of 4146 km and a pointing accuracy of 1 mrad, the control frequency  $f_c$  is 0.0036 Hz. There seems to be adequate margin unless the damping is very low — which it may be.
- The slenderness ratio of the compression members is less than 300.
- Meteoroid damage would be of great concern. The detail design of the many tension members should incorporate multifilar redundancy.

More investigation is needed, of course, but the approach of designing the structure to give adequate stiffness to the membrane to meet precision requirements results in a viable configuration.

### CONCLUDING REMARKS

The topic of this study is one of immense depth and breadth. The work accomplished provides a valuable insight into the design process for large space structures, as well as a base for future, more detailed studies. Based on this work, the conclusion is that the most critical design requirements arise from the necessity of providing sufficient dimensional refinement, accuracy, and stability.

## REFERENCES

1. Hedgepeth, John M.; and Miller, Ronald R.: Effect of Member-Length Imperfections on the Deformations and Loads in an Isogrid-Truss Structure. *Journal of Solids and Structures* (to be published).
2. Hedgepeth, John M.: Influence of Fabrication Tolerances on the Surface Accuracy of Large Antenna Structures. *AIAA Journal* (to be published).
3. Hedgepeth, John M.: Accuracy Potentials for Large Space Antenna Structures. SAWE Paper No. 1375. Presented at the 39th Annual Conference of the Society of Allied Weight Engineers, Inc., St. Louis, MO, 12-14 May 1980.
4. Hedgepeth, John M.: Influence of Interorbit Acceleration on the Design of Large Space Antennas, Large Space Systems/Low-Thrust Propulsion Technology. NASA CP-2144, pp. 157-178, 1980.
5. Hedgepeth, John M.: Design Concepts for Large Antenna Reflectors. Large Space Systems Technology - 1980, Volume II - Base Technology, Frank Koprivier III, compiler. NASA CP-2168, 1980, pp. 103-119.
6. Hedgepeth, John M.: Free-Flying Solar-Reflector Spacecraft, Large Space Systems Technology - 1980, Volume II - Base Technology, Frank Koprivier III, compiler. NASA CP-2168, pp. 89-101, 1980.
7. Hedgepeth, John M.; Knapp, Karl K.; and Finley, Laurence A.: Structural Design of Free-Flying Solar-Reflecting Satellites. SAWE Paper No. 1303. Presented at the 38th Annual Conference of the Society of Allied Weight Engineers, Inc., New York, NY, 7-9 May 1979.
8. Garrett, Henry B.; and Pike, Charles P., eds: Space Systems and Their Interactions with Earth's Space Environment. *Progress in Astronautics and Aeronautics*, vol. 71, 1980, AIAA.
9. Hedgepeth, John M.; Miller, Richard K.; and Knapp, Karl: Conceptual Design Studies for Large Free-Flying Solar-Reflector Spacecraft. NASA CR-3438, 1981.
10. Bush, Harold, G.; Mikulas, Martin M.; and Heard, Walter L.: Some Design Considerations for Large Space Structures. Presented at the AIAA/ASME 18th Structures, Structural Dynamics, and Materials Conference, San Diego, CA, 21-23 March 1977, Paper No. 77-395.
11. Hedgepeth, John M.; MacNeal, Richard H.; Knapp, Karl; and MacGillivray, Charles S.: Considerations in the Design of Large Space Structures. NASA CR-165744, 1981.
12. Coyner, John V.; Hedgepeth, John M.; and Riead, Harry D.: Long-Boom Concepts. NASA CR-145169, September 1977.

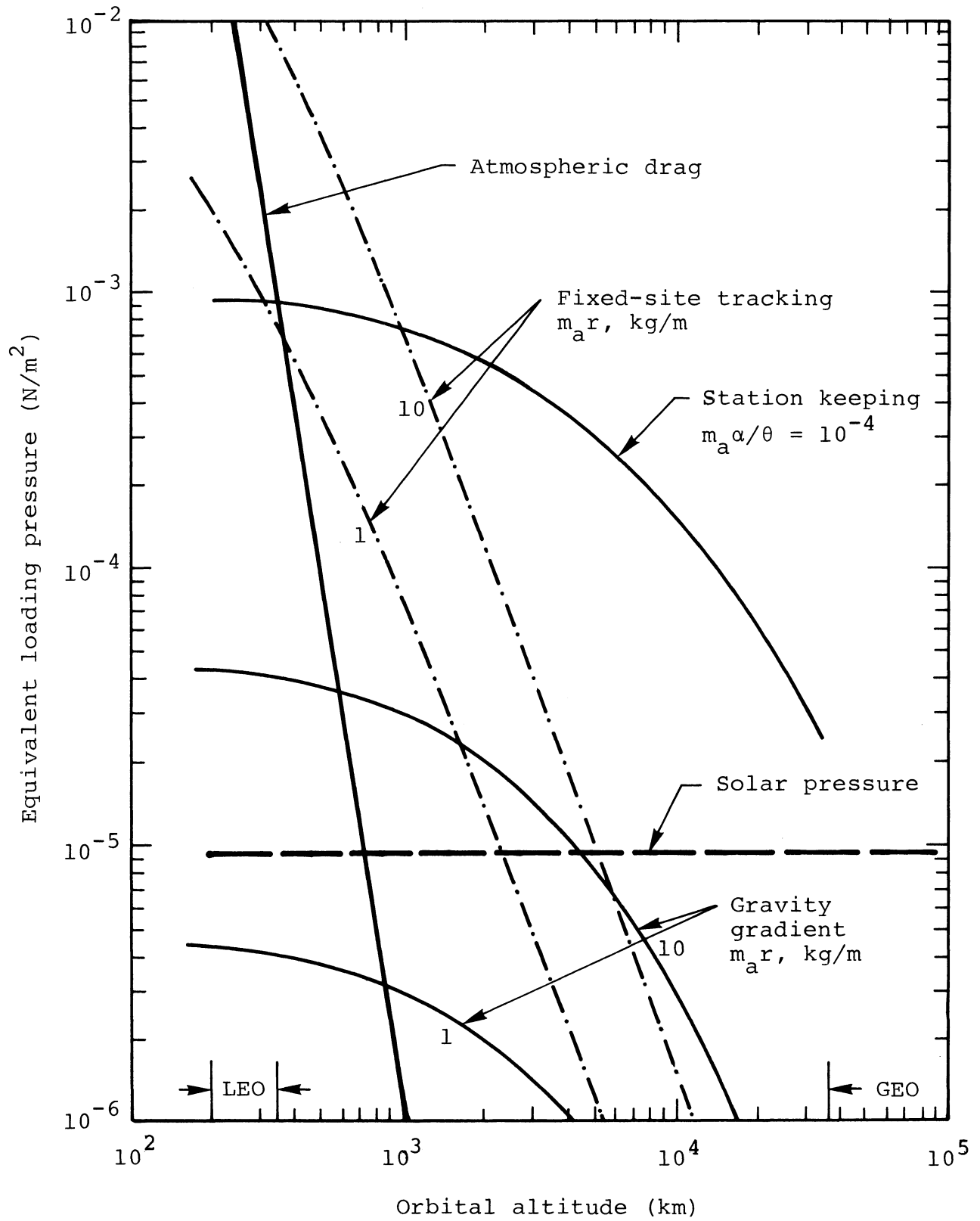


Figure 1.- Equivalent loading pressure versus orbital altitude.

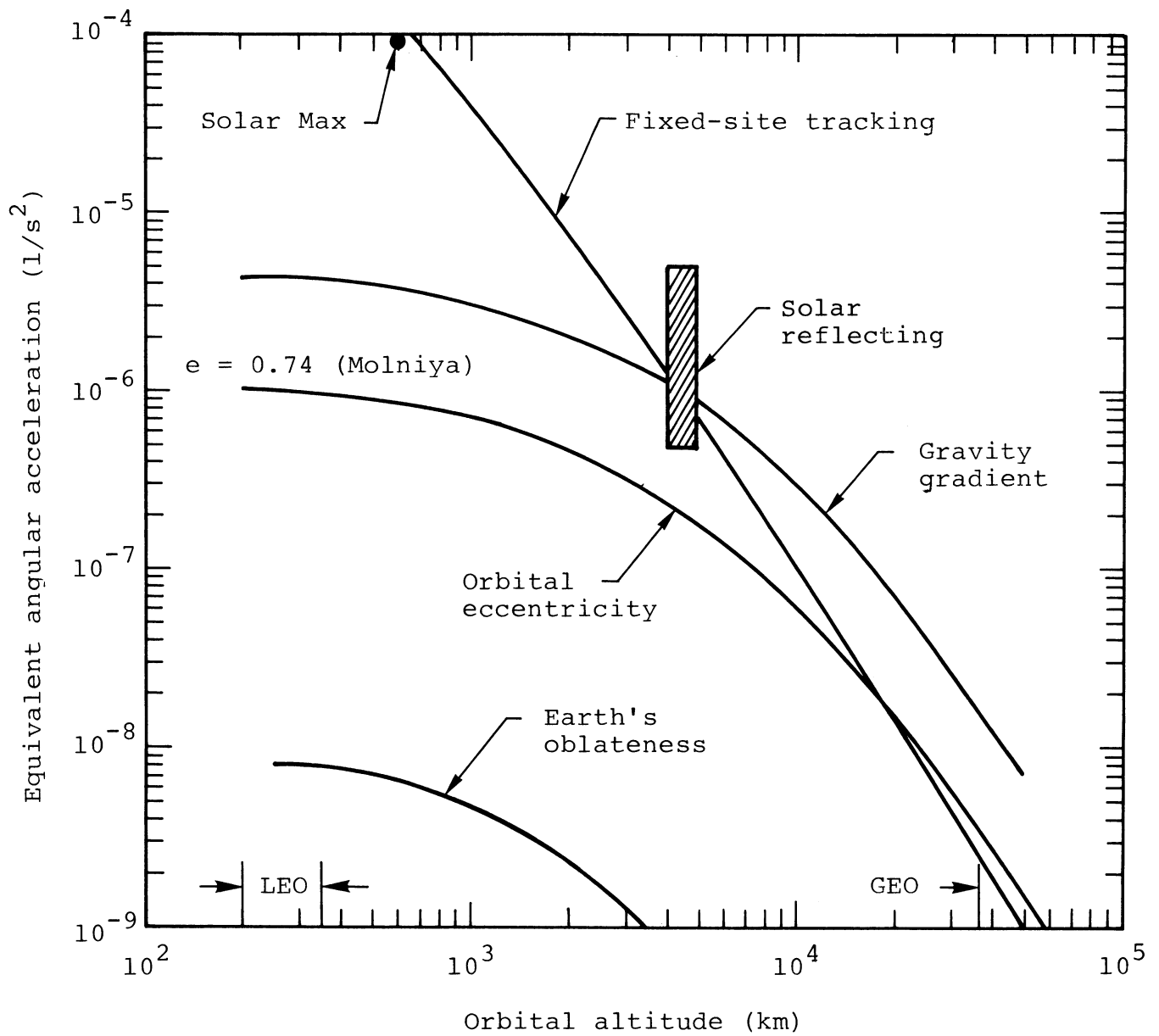


Figure 2.- Equivalent angular acceleration versus orbital altitude.

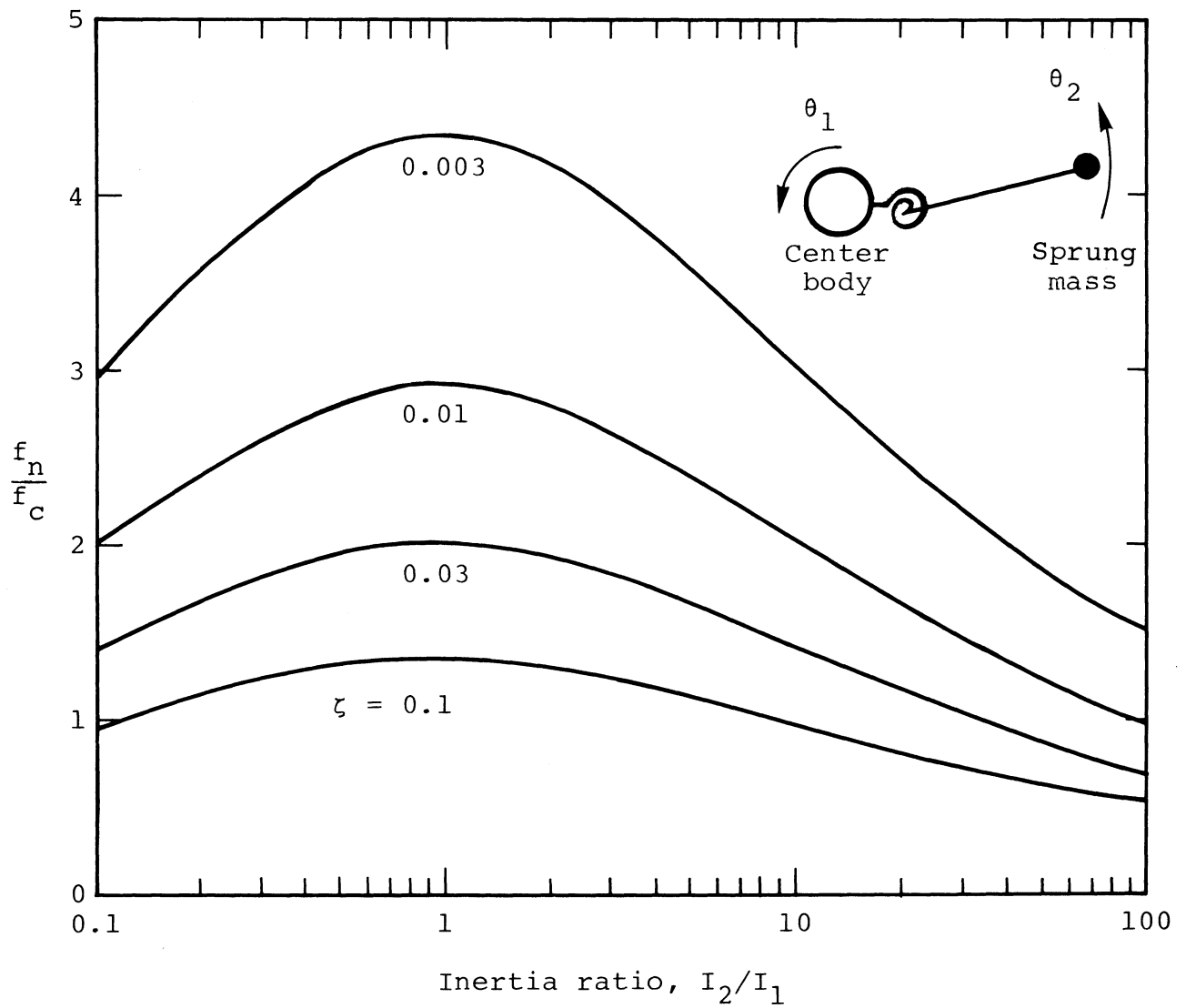
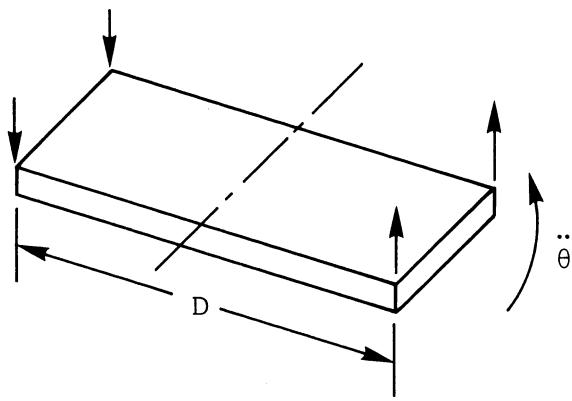
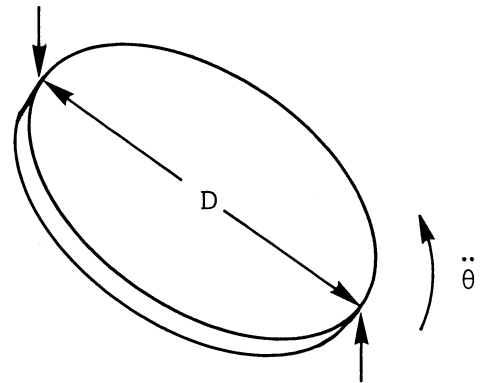


Figure 3.- Required frequency ratio for stability for a center-body controlled spacecraft with flexible appendages. Rolloff = 6 dB/octave.



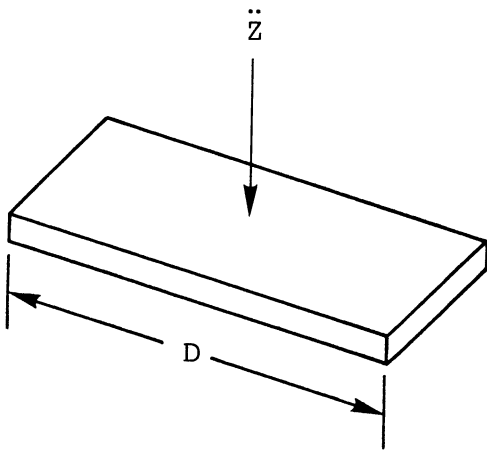
$$\Gamma_{\theta} = 0.95 \times 10^{-3}$$



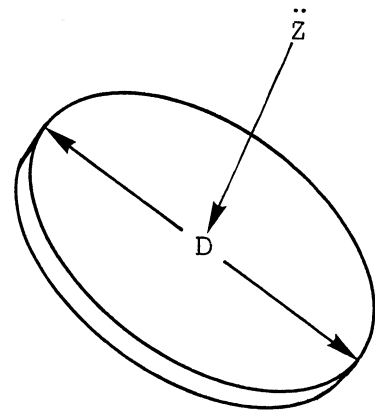
$$\Gamma_{\theta} = 2.14 \times 10^{-3}$$

$$\frac{w_{\text{rms}}}{D} = \Gamma_{\theta} \frac{\ddot{\theta}}{f_n^2}$$

Figure 4.- Deformations due to attitude control.



$$\Gamma_Z = 12.2 \times 10^{-3}$$



$$\Gamma_Z = 25.1 \times 10^{-3}$$

$$w_{\text{rms}} = \Gamma_Z \frac{\ddot{Z}}{f_n^2}$$

Figure 5.- Deformations due to lateral acceleration.

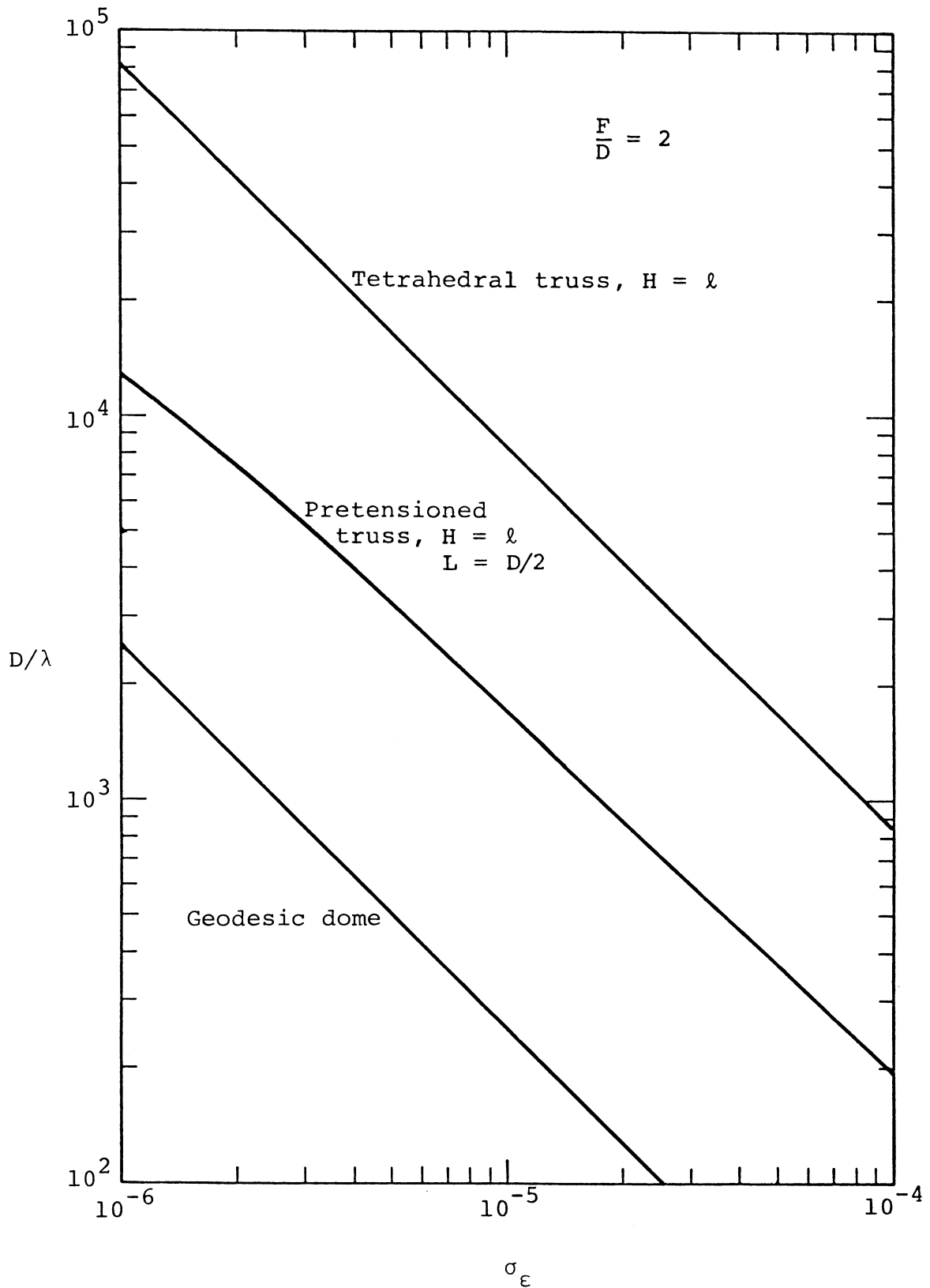


Figure 6.- Potential antenna sizes for  $w_{rms} = \lambda/100$  as limited by fabrication imperfections.

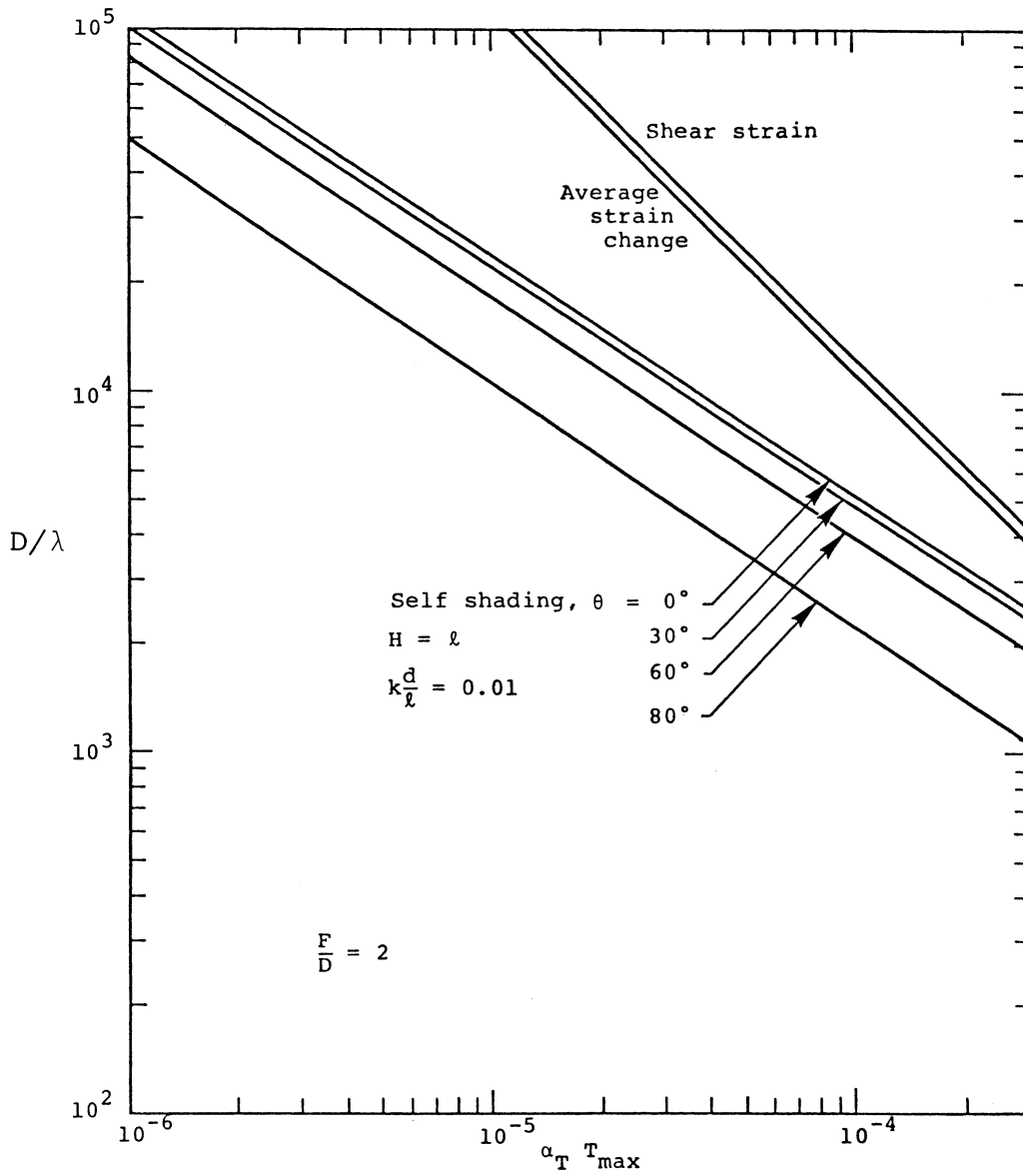


Figure 7.- Potential tetrahedral truss antenna size for  $w_{rms} = \lambda/100$  as limited by thermal strains.

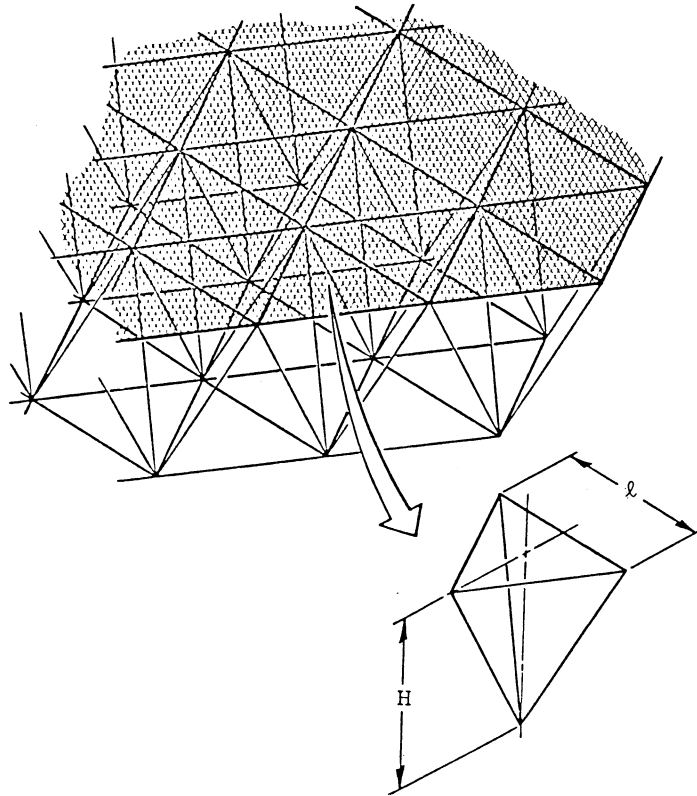
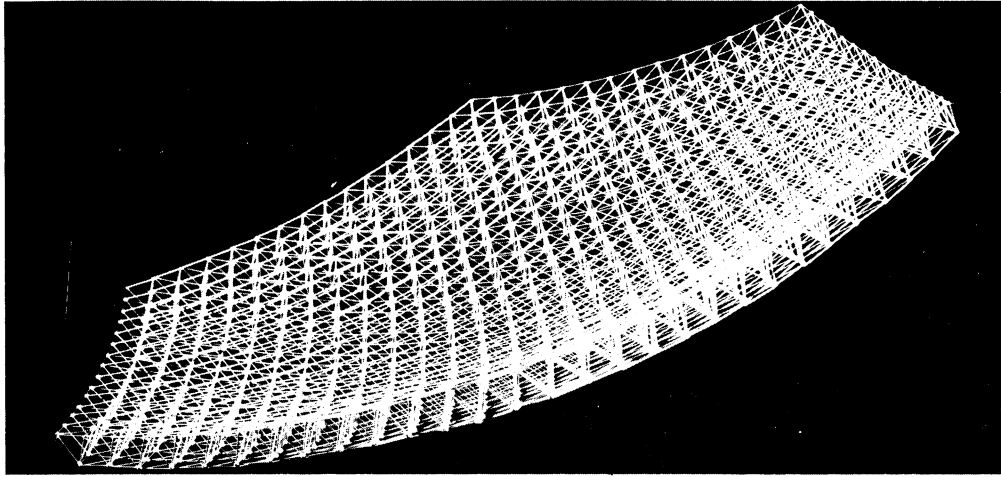


Figure 8.- Tetrahedral truss configuration.

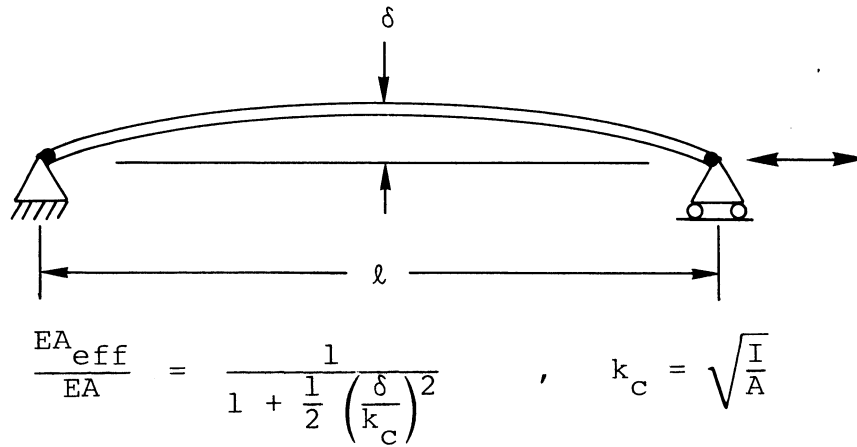
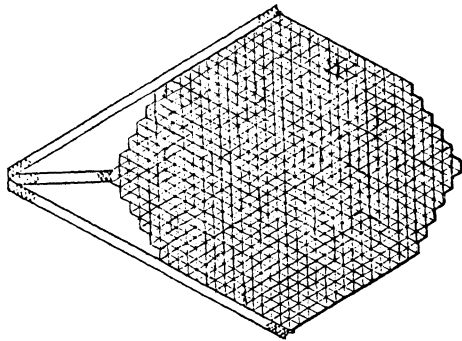


Figure 9.- Effect of out-of-straightness on axial stiffness.

$l/k_c <$	CASE
$\frac{573.9}{l^{1/3}}$	Horizontal testing. Gravity sag $< k_c/3$
$\frac{2700}{l^{1/2}}$	Vertical testing. Tension $< 1/10$ Euler load
1633	Fabrication. $\Delta\epsilon = 10^{-6}$
414	Built-in loads $< 1/10$ Euler load, $\sigma_\epsilon = 10^{-5}$
$2.8 \frac{D^2}{Hl}$	Member vibration frequency $> 3$ truss frequency, $m_p/m_2 = 2, k = 2$

Figure 10.- Allowable member slenderness. Length  $l$  is in meters. Member density = 1520 kg/m<sup>3</sup>; Young's modulus = 110 GPa.



Cell size = 7 m  
Depth = 7 m  
Strut size = 40-mm dia. x 0.35-mm wall  
Reflector mass = 6500 kg  
Vibration frequency (reflector only)  
approximately equals 1 Hz  
Surface error  $\approx$  4 mm

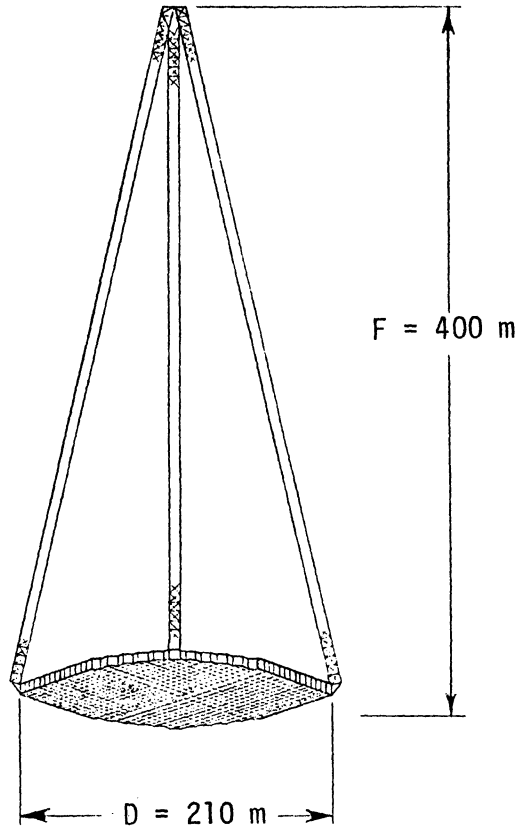
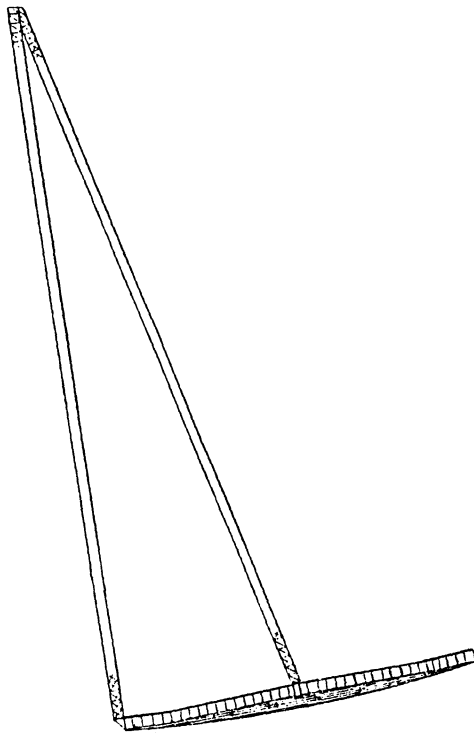


Figure 11.- 200-m-diameter deployable antenna.

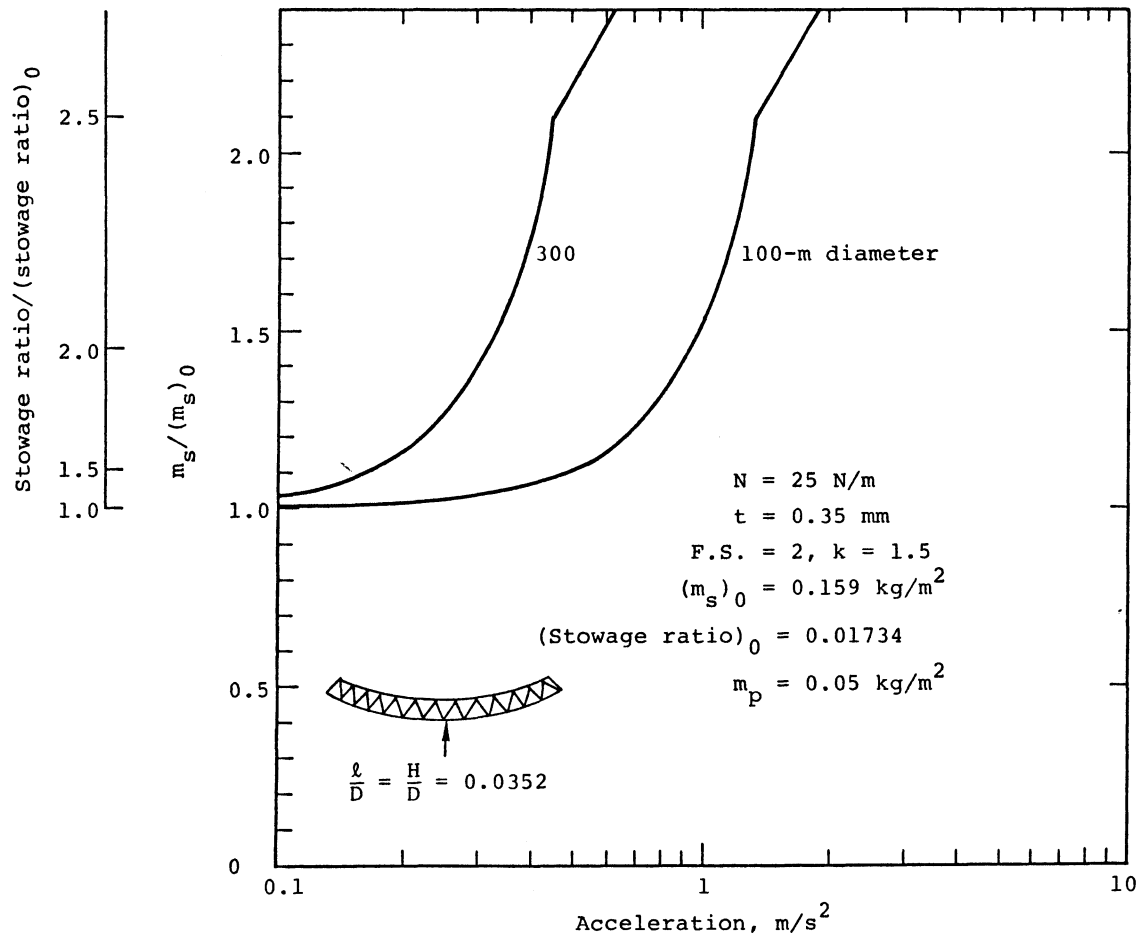


Figure 12.- Mass and stowage ratio for tetrahedral truss.

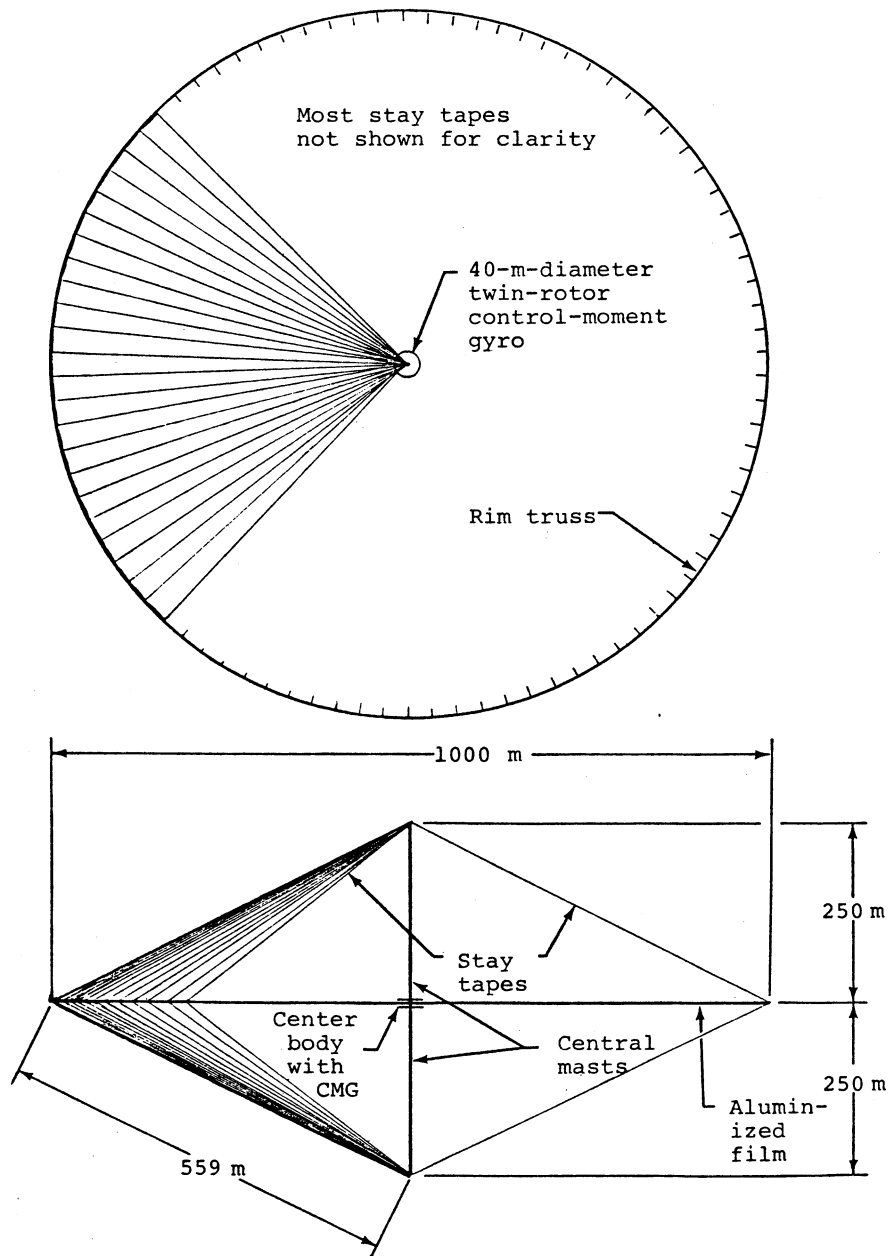


Figure 13.- Baseline configuration of a solar-reflector spacecraft.

## APPENDIX

### FLEXIBLE-STRUCTURE ANALYSES

This section contains otherwise unpublished analyses of flexible structures, the results of which are reported in the body of this paper.

#### Structure-Control Interaction for a Uniform Beam

The analysis of reference 12 is based on a model in which tip masses are connected by massless structure to a central spacecraft body. For many future situations, the masses and flexibilities will be distributed over the entire spacecraft. An appropriate simple model might then be a uniform beam.

The analysis of reference 12 further reflects present design practice in treating only the situation in which the attitude is sensed at the central body and corrective moments are applied to it. Future control systems may sense attitude by tracking the displacements of the tips and apply corrective moments by means of tip-mounted thrusters. These alternatives require analysis.

Consider the motion of a free-free beam of length  $L$  rolling about its center. Let the deflection of the beam be given by

$$y = \theta x + ay_1(x)$$

where  $x$  is the coordinate along the beam from its center and  $y_1$  is the first antisymmetric free-free uniform-beam mode normalized so that

$$\int_{-L/2}^{L/2} y_1^2(x) dx = L$$

The motion is then described by the generalized coordinates  $\theta$  and  $a$  where  $\theta$  is the mean rotation and  $a$  is the amplitude of the bending displacement.

Let  $Q$  be the torque applied by the attitude control system. Then the equations of motion can be written

$$I\ddot{\theta} = Q$$

$$M\left(\ddot{a} + \zeta \frac{\omega_1^2}{\omega_n} \dot{a} + \omega_1^2 a\right) = Q \frac{dy_1}{dx}(0) \quad , \quad \text{for center torquing}$$

$$= \frac{2Q}{L} y_1\left(\frac{L}{2}\right) \quad , \quad \text{for tip torquing}$$

where  $M$  is the mass of the beam,  $I$  is its moment of inertia,  $\omega_1$  is the first free-free antisymmetrical frequency, and  $\omega_n$  is the natural frequency of the beam cantilevered in the center.

Note that damping has been included where  $\zeta$  is the reciprocal of the resonant amplification factor for cantilever forced vibrations. In the Laplace-transform plane, the equations of motion become

$$\theta = \frac{Q}{Ip^2}$$

$$a = \frac{Q}{M\left(p^2 + \zeta \frac{\omega_1^2}{\omega_n} p + \omega_1^2\right)} \frac{dy_1}{dx}(0) \quad , \quad \text{for center torquing}$$

$$= \frac{Q}{M\left(p^2 + \zeta \frac{\omega_1^2}{\omega_n} p + \omega_1^2\right)} \frac{y_1\left(\frac{L}{2}\right)}{L/2} \quad , \quad \text{for tip torquing}$$

Assume the control law to be

$$Q = I\omega_c^2 R(p)\bar{\theta}$$

where  $\omega_c$  is the control frequency in radians per second (see Eq. (2)),  $R$  is the rolloff function (see ref. 12), and  $\bar{\theta}$  is the sensed angle error.

$$\bar{\theta} = \theta + a \frac{dy_1}{dx}(0) \quad , \quad \text{for center sensing}$$

$$= \theta + a \frac{y_1\left(\frac{L}{2}\right)}{L/2} \quad , \quad \text{for tip sensing}$$

Combining the equations gives

$$\bar{\theta} = \frac{\omega_c^2}{p^2} R(p) \left[ 1 + \frac{4I p^2}{ML^2 \left( p^2 + \zeta \frac{\omega_1}{\omega_n} p + \omega_1^2 \right)} F \right] \bar{\theta}$$

where

$$F = \left[ \frac{L}{2} \frac{dy_1}{dx}(0) \right]^2 \quad , \quad \text{for center torquing and sensing}$$

$$= \left[ y_1\left(\frac{L}{2}\right) \right]^2 \quad , \quad \text{for tip torquing and sensing}$$

$$= \frac{L}{2} y_1\left(\frac{L}{2}\right) \frac{dy_1}{dx}(0) \quad , \quad \text{for center-tip combination}$$

Applying the reasoning of reference 12 yields the condition for gain stability

$$\left(\frac{\omega_1}{\omega_c}\right)^{2+r} > \frac{|F|}{3\zeta \frac{\omega_1}{\omega_n}}$$

In terms of cantilever quantities, the condition is

$$\left(\frac{\omega_n}{\omega_c}\right)^{2+r} > \frac{|F|}{3\left(\frac{\omega_1}{\omega_n}\right)^{3+r}} \frac{1}{\zeta}$$

For the first antisymmetric uniform-beam mode,

$$y_1\left(\frac{L}{2}\right) = 2$$

$$\frac{L}{2} \frac{dy_1}{dx}(0) = -5.401$$

Also, the ratio  $\omega_1/\omega_n$  is

$$\frac{\omega_1}{\omega_n} = 4.38$$

Thus, the requirement for frequency ratio (in Hertz) is

$$\left(\frac{f_n}{f_c}\right)^{2+r} > \frac{C}{(4.38)^{3+r}} \frac{1}{\zeta}$$

where C is given in the following table.

	TORQUING		
		CENTER	TIP
SENSING			
Center		9.7	3.6
Tip		3.6	1.333

### Distortions Due to Steady Angular Accelerations

Consider a beam of length  $D$  (see Figure 4) with tip-applied forces causing an angular acceleration of  $\ddot{\theta}$ . The force at each tip is

$$P = \frac{mD^2}{12} \ddot{\theta}$$

where  $m$  is the mass per unit length of the beam.

The acceleration causes an equilibrating d'Alembert inertia loading per unit length

$$p = mx \ddot{\theta}$$

where  $x$  is the distance from the center.

The loading distorts the beam into the shape

$$w = \frac{mD^5 \ddot{\theta}}{720 EI} \left[ 5 \left( \frac{x}{D} \right)^3 - 6 \left( \frac{x}{D} \right)^5 \right]$$

where  $EI$  is the bending stiffness.

Determining the rms departure from a best-fit straight line gives

$$\frac{w_{rms}}{D} = 1.89 \times 10^{-4} \frac{mD^4}{EI} \ddot{\theta}$$

But, if the beam is clamped in the center, the cantilever natural frequency is

$$f_n = \frac{3.52}{2\pi} \sqrt{\frac{EI}{m\left(\frac{D}{2}\right)^4}}$$

Combining the two equations gives

$$f_n^2 = 9.5 \times 10^{-4} \frac{\ddot{\theta}}{\frac{w_{rms}}{D}}$$

for the required natural frequency to maintain the desired accuracy.

In a similar fashion, consider a circular plate of diameter  $D$  with rim forces producing a roll rate of  $\ddot{\theta}$  (see Figure 4). The value of rim force is

$$P = \frac{\pi D^3}{64} m \ddot{\theta}$$

where  $m$  is the mass per unit area. The equilibrating d'Alembert force per unit area is

$$p = mr \cos \phi \ddot{\theta}$$

where  $r$  and  $\phi$  are polar coordinates.

The plate deflection  $w$  satisfies the following boundary-value problem

$$D_p \nabla^4 w = p, \quad r < a$$

$$\left. \begin{aligned} \frac{\partial^2 w}{\partial r^2} + \nu \left( \frac{1}{r} \frac{\partial w}{\partial r} + \frac{1}{r^2} \frac{\partial^2 w}{\partial \phi^2} \right) &= 0 \\ - D_p \left[ \frac{\partial}{\partial r} \nabla^2 w + \frac{1-\nu}{r} \frac{\partial}{\partial r} \left( \frac{1}{r} \frac{\partial^2 w}{\partial \phi^2} \right) \right] &= \frac{P}{D/2} [\delta(0) - \delta(\pi)] \end{aligned} \right\} r = a$$

where  $D_p$  is the plate stiffness,  $\nu$  is Poisson's ratio, and  $\delta$  is the Dirac delta function.

The solution can be obtained by setting

$$w = \sum_{n=0}^{\infty} W_n(r) \cos n\phi$$

and substituting into the differential equation and boundary conditions. The rms value is then obtained by summing as follows:

$$\overline{w^2} = \frac{1}{(D/2)^2} \sum_{n=0}^{\infty} \int_0^{D/2} W_n^2(r) r dr$$

where, of course, the function  $W_1(r)$  is adjusted by subtracting enough rigid-body displacement to make the difference represent the departure from the best-fit plane.

Performing the steps is straightforward, albeit arduous, especially for  $n=1$ . The infinite summation is readily approximated since the series converges as the fifth power of  $(1/n)$ . The resulting expression for the rms distortion for  $\nu = 1/3$  is

$$\frac{w_{\text{rms}}}{D} = 3.3 \times 10^{-4} \frac{mD^4}{D_p} \ddot{\theta}$$

The natural frequency of a plate cantilevered from its centerline can be estimated by calculating the Rayleigh quotient for the mode shape

$$w = r^2 \cos^2 \phi$$

The result is

$$f_n = \frac{8}{\pi} \sqrt{\frac{D_p}{mD^4}}$$

Combining the two equations yields

$$f_n^2 = 2.14 \times 10^{-3} \frac{\ddot{\theta}}{\frac{w_{rms}}{D}}$$

as the stiffness requirement to maintain the desired accuracy.

#### Distortions Caused by Lateral Acceleration

Consider a beam of length D with a central force causing a lateral acceleration of  $\ddot{Z}$ . The value of the force is

$$P = mD\ddot{Z}$$

where m is the mass per unit length. The equilibrating d'Alembert inertia load per unit length is

$$p = m\ddot{Z}$$

The distortion of the beam is given by

$$w = \frac{mD^4\ddot{Z}}{48EI} \left[ 3\left(\frac{x}{D}\right)^2 - 4\left(\frac{x}{D}\right)^3 + 2\left(\frac{x}{D}\right)^4 \right]$$

where EI is the bending stiffness and x is the distance from the center of the beam.

Determining the rms deviation from the best-fit straight line gives

$$w_{\text{rms}} = 2.43 \times 10^{-3} \frac{mD^4}{EI} \ddot{z}$$

This can be expressed in terms of the natural frequency of the beam cantilevered in the center

$$w_{\text{rms}} = 12.2 \times 10^{-3} \frac{\ddot{z}}{f_n^2}$$

For a circular plate accelerated by a force at the center, a similar process yields

$$w_{\text{rms}} = 3.86 \times 10^{-3} \frac{mD^4}{D_p} \ddot{z}$$

Expressed in terms of the approximate semiplate cantilever frequency, this yields

$$w_{\text{rms}} = 25.1 \times 10^{-3} \frac{\ddot{z}}{f_n^2}$$

1. Report No. NASA CR-3484	2. Government Accession No.	3. Recipient's Catalog No.	
4. Title and Subtitle CRITICAL REQUIREMENTS FOR THE DESIGN OF LARGE SPACE STRUCTURES		5. Report Date November 1981	6. Performing Organization Code
		8. Performing Organization Report No. ARC-R-1016	10. Work Unit No.
7. Author(s) John M. Hedgepeth		11. Contract or Grant No. NAS1-15347	13. Type of Report and Period Covered Contractor Report
9. Performing Organization Name and Address Astro Research Corporation 6390 Cindy Lane Carpinteria, CA 93013		14. Sponsoring Agency Code	
		12. Sponsoring Agency Name and Address National Aeronautics and Space Administration Washington, D.C. 20546	
15. Supplementary Notes Langley Technical Monitor: Melvin S. Anderson Final Report			
16. Abstract  The future promises large structures which must be deployed, erected, assembled, or fabricated in space. Such structures will be designed to deal with phenomena as primary criteria which have been considered as only secondary in the past. The purpose of this paper is to discuss these spaceflight design requirements. The conclusion is reached that for most situations, the primary requirements will arise from the demands for high dimensional accuracy of the structure throughout its long useful life.			
17. Key Words (Suggested by Author(s)) Advanced concepts Spaceflight loads Structural precision Stiffness requirements		18. Distribution Statement  Unclassified - Unlimited  Subject Category 18	
19. Security Classif. (of this report) Unclassified	20. Security Classif. (of this page) Unclassified	21. No. of Pages 48	22. Price A03

For sale by the National Technical Information Service, Springfield, Virginia 22161

NASA-Langley, 1981